AIAA 98-0683

HYPERSONIC FLOW OVER A FLAT PLATE

P.G.P. Toro,§ Z. Rusak,ɔ L. N. Myrabo,† and H.T. Nagamatsu,‡
Department of Mechanical Engineering, Aeronautical Engineering, and Mechanics
Rensselaer Polytechnic Institute, Troy, NY 12180-3590

ABSTRACT

The viscous boundary layer flow near the leading edge of a flat plate given in supersonic and hypersonic speeds is numerically investigated. The boundary layer and shock wave may merge near the leading edge depending on the Mach number, Reynolds number and wall temperature. We consider air as calorically perfect gas, with a constant Prandtl number and Sutherland's law for the viscosity. The two-dimensional Navier-Stokes equations for a non-steady flow, with no body forces, no volumetric heating and no mass diffusion are solved using the explicit finite-difference MacCormack's time marching technique. Solutions for the flow parameters such as the boundary layer thickness, the pressure profile in both directions (x and y directions), the streamwise velocity profile and the temperature and density distributions over a flat plate with constant surface temperature are presented. The numerical results are also compared with recent similarity solutions for supersonic laminar boundary layers that use a general power law for the viscosity-temperature relation. Nice agreement between the solutions is found at the trailing edge of the plate. As Mach number increases, longer distance is needed for the boundary layer to establish a self-similar structure.

---

§ Graduate Student, AIAA Student Member.

ɔ Associate Professor of Aeronautical Engineering, AIAA senior Member.

† Associate Professor of Engineer Physics, AIAA Member.

‡ Active Professor Emeritus of Aeronautical Engineering, AIAA Fellow.

INTRODUCTION

The development of modern hypersonic space vehicles requires knowledge regarding the characteristics of hypersonic flows in the immediate vicinity of a leading edge of lifting surfaces. Under certain conditions, the boundary layer may remain laminar over some distance of the vehicle. The laminar boundary layers may be expected in hypersonic flights at high altitudes, where the density, and hence the Reynolds number per unit length, is relatively low. Sternberg[1] observed laminar boundary layers at Reynolds numbers as high as 5 x 10^7 in flight tests of the V-2 rocket. Van Driest[2] showed theoretically that when the solid boundary is sufficiently cooled, the laminar boundary layer may be stabilized regardless of Reynolds number at Mach numbers from 1 to 9.

Sharp flat plates have been used to investigate the shock wave and boundary layer formation in rarefied to continuum flow conditions in several experimental facilities. Experimental results[3-6] at supersonic speeds and rarefied free stream conditions have indicated the existence of the slip region near the leading edge. Also, the experimental results[5] indicate that in a continuum flow, when Mach number is much higher than 1, slip can take place along a limited region of the flat plate near the leading edge of the length ζ. They also show that there exists a delay in the formation of the maximum shock wave angle and the boundary layer near the leading edge. This delay in formation is caused by the slip phenomena in the close vicinity of the leading edge.[5-6] After the slip region in the continuum gas over a flat plate, the shock wave and the boundary layer may merge along some distance before separating.[5] Both the formation and the delay in the maximum shock wave angle and the boundary layer are strongly influenced by the free stream Mach number, M, the Knudsen number, Kn (ratio of the mean free path, λ, to the leading edge thickness, t), and the Reynolds number, Re_t, based upon the leading edge thickness.

For flows with Knudsen number much less than unity, a detached shock wave forms in front of the plate and the flow after the normal shock is

subsonic with relatively high pressure. Consequently, there is no possibility of the existence of slip flow for a reasonably dense gas. In this case, the viscous effects become small and the inviscid flow over the leading edge predominates.[7, 8]

From first order kinetic theory it can be shown that the no slip flow may be found when $\left(\frac{Re_\zeta}{M^2}\right) \geq N$. Here N is the number of intermolecular collisions, Re_ζ is Reynolds number based on the slip distance, ζ, and M is the free stream Mach number. It can be seen that ζ increases as M is increased.

A hypersonic flow over a flat plate may be divided into four distinct regions, Figure 1.

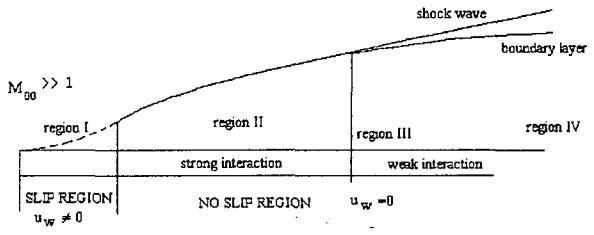

Figure 1. Flowfield on a flat plate at hypersonic flow.

Starting from the leading edge of the plate, hypersonic flow with slip phenomena on the plate is formed. In this region the flow is not continuum, the Navier-Stokes equations are not valid and the first order kinetic flow theory may take place.[6] Immediately, after the noncontinuum region, in the strong interaction region, the flow can be considered as continuum. In this region the shock wave and the boundary layer are merged[5, 6, 9] with a no slip flow condition on the surface of the plate.

It should be noticed that in the lower supersonic speed regime the boundary layer and shock wave are so far apart that their interaction effects can probably be neglected.[10, 11] However, the situation is quite different when a hypersonic speed is reached. Since the shock wave angle is proportional to $1/M$, it is so close to the flat plate surface that the entire region between the shock wave and the surface should be considered as a viscous flow layer. Consequently, viscous effects must be considered in the determination of the shock wave and the boundary layer characteristics in the strong interaction region. Also, in this region the pressure gradient in the y-direction may be ignored, $\frac{\partial p}{\partial y} \equiv 0$, but the pressure gradient in the x-direction can not be neglected, due to the presence of the shock wave inside the viscous layer.

Li and Nagamatsu[9] developed a theory for the hypersonic strong interaction between shock wave and boundary layer for an insulated sharp flat plate in continuum, perfect gas flow. They considered that, starting from the leading edge, the shock wave and boundary layer are merged with no slip flow on the plate and the Knudsen number equals unity. This theory is not valid in the rarefied flow region with slip velocity condition. Thin thickness of the shock wave was assumed. The flow variables in the region bounded by the shock wave and the plate surface was solved using the compressible laminar boundary layer equations. Due the presence of the viscous layer, a fictitious curvature effects was considered by $\frac{\partial p}{\partial x} = \frac{dp_2}{dx}$ in both momentum and energy equations. The equations were solved with the no slip and no penetration flow conditions at the insulated wall. Also the free stream properties and the flow behind the shock wave was matched. Finally, at the edge of the outer viscous layer the pressure jump across the oblique shock must be satisfied.

Later, Li and Nagamatsu[12] developed the similar solutions for the compressible boundary layer flow. For a perfect gas with unit Prandtl number and dynamic viscosity as a linear function of temperature, the momentum and energy equations are reducible to ordinary differential equations. Li and Nagamatsu[13] extended their formulation for a noninsulated flat plate.

Recently, several numerical codes have been developed to study the strong interaction of a shock wave and boundary layer in laminar hypersonic flow over a flat plate. The Reynolds averaged Navier-Stokes equations were solved by Nagamatsu et al.,[14] using the PARC2D code.[15] In this work, the dynamic viscosity was determined by Sutherland's law. Anderson[11] has applied the explicit finite-difference MacCormack's time marching technique to the Navier-Stokes equations in a two-dimensional, non-steady flow with no body forces, no volumetric heating and no mass diffusion. He assumed the no-slip condition on the wall and the free stream pressure and temperature at the stagnation point of the leading edge of the plate rather than conditions behind a shock wave.

Far from the leading edge region, a weaker interaction region may be found, Figure 1. In this

region, which is close to the strong interaction region the pressure gradients in the x- and y-directions inside the boundary layer are small and may be ignored. However, outside the boundary layer, in the inviscid layer between the shock wave and the boundary layer, the pressure gradient in the y-direction can not be neglected. Therefore, downstream of the strong interaction region, the classical approach of Prandtl's incompressible boundary layer theory may be applied to the compressible boundary layer.

Van Driest[16] used Crocco's method and derived a set of ordinary differential equations to describe a self-similar compressible laminar boundary layer. He studied flows with free stream Mach numbers up to 25 over a flat plate, assuming a perfect gas obeying Sutherland's viscosity law. Results on the skin-friction and heat-transfer coefficients as function of Reynolds number, Mach number, and wall-to-free stream temperature ratio were presented.

The laminar boundary layer equations for compressible supersonic and hypersonic flows over an adiabatic sharp flat plate were numerically solved by Moraes et al.[17] using a finite element method.

Recently, Toro et al.[18] have proposed a new method of deriving a self-similar solution of the compressible laminar boundary layer equations. Air was considered as calorically or thermally perfect gas and the viscosity as a power function of the temperature. Modified Levy-Mangler and Dorodnitsyn-Howarth transformations have been introduced to solve the flow in a thin laminar boundary layer on a smooth flat plate with no external pressure gradient. These transformations describe the similarity variable in terms of a power of the density that takes into account the viscosity-temperature power law relation. This results in an explicit relation between the stream function and the temperature fields described by a closed coupled system of nonlinear ordinary differential equations. This new methodology was used to numerically investigate the air flow in two different situations: a hypersonic fluid flow over a flat plate,[18] and a hypersonic fluid flow induced by a shock wave advancing into a stationary fluid bounded by a solid wall.[19]

In the present paper the strong interaction between a shock wave and an boundary layer, in a hypersonic viscous flow, close to the leading edge of the flat plate is numerically investigated. We ignore the small slip region. The explicit finite-difference MacCormack's scheme is used to solve the full Navier-Stokes equations.

The computed flow behavior downstream of the strong interaction region is compared with the self-similar solution of Toro et al.[18]

MATHEMATICAL MODEL

Ignoring the relatively small slip region, where the Navier-Stokes equations are not valid, and considering that a laminar boundary layer starts at the leading edge and remains laminar along the plate, the two-dimensional, non-steady flow with no body forces, no volumetric heating and no mass diffusion can be described, in conservative vector form, by

$$\frac{\partial U}{\partial t}+\frac{\partial E}{\partial x}+\frac{\partial F}{\partial y}=0 \qquad (1)$$

A full Navier-Stokes analysis is be expected to yield a complete solution for a continuum flow near the leading edge of a flat plate. Here U is a solution column vector , E and F are flux terms column vectors, given by

$$U=\begin{Bmatrix}\rho\\ \rho u\\ \rho v\\ E_t\end{Bmatrix},$$

$$E=\begin{Bmatrix}\rho u\\ \rho uu+p-\tau_{xx}\\ \rho uv-\tau_{xy}\\ (E_t+p)u+q_x-u\tau_{xx}-v\tau_{xy}\end{Bmatrix},$$

$$F=\begin{Bmatrix}\rho v\\ \rho vu-\tau_{yx}\\ \rho vv+p-\tau_{yy}\\ (E_t+p)v+q_y-u\tau_{yx}-v\tau_{yy}\end{Bmatrix}. \qquad (2)$$

The viscous terms are given by:

$$\tau_{xx}=\lambda\left(\nabla.\vec{V}\right)+2\mu\frac{\partial u}{\partial x},$$

$$\tau_{yy}=\lambda\left(\nabla.\vec{V}\right)+2\mu\frac{\partial v}{\partial y},$$

$$\tau_{xy} = \tau_{yx} = \mu\left(\frac{\partial u}{\partial y} + \frac{\partial v}{\partial x}\right),$$

$$q_x = -k\frac{\partial T}{\partial x}, \qquad q_y = -k\frac{\partial T}{\partial y},$$

$$\lambda = -\frac{2}{3}\mu. \tag{3}$$

The total energy is given by

$$E_t = \rho\left(e + \frac{|\vec{V}|^2}{2}\right) \tag{4}$$

The velocity vector and the absolute values of the velocity are given by

$$\vec{V} = u\vec{i} + v\vec{j}, \quad |\vec{V}| = \sqrt{u^2 + v^2} \tag{5}$$

For a caloricaly perfect gas, the relation between the internal energy and specific heat at constant volume and pressure may be calculated by

$$p = \rho RT, \qquad e = c_v T,$$

$$c_v = \frac{R}{\gamma - 1}, \qquad c_p = \gamma c_v \tag{6}$$

The viscosity and thermal conductivity are given by Sutherland's law:

$$\mu = \frac{1.458.10^{-6}T^{3/2}}{T + 110.4}, \qquad k = \frac{\mu c_p}{Pr} \tag{7}$$

MacCormack's TECHNIQUE

The explicit finite-difference MacCormack's time marching technique is applied. The MacCormack's technique is a second-order-accurate in both space and time[11, 20] and it is given by

$$U_{i,j}^{t+\Delta t} = U_{i,j}^{t} + \left(\frac{\partial U}{\partial t}\right)_{av} \Delta t \tag{8}$$

where

$$\left(\frac{\partial U}{\partial t}\right)_{av} = \frac{1}{2}\left[\left(\frac{\partial U}{\partial t}\right)_{i,j}^{t} + \left(\frac{\partial \overline{U}}{\partial t}\right)_{i,j}^{t+\Delta t}\right] \tag{9}$$

Figure 2 shows the grid points for the time marching technique.

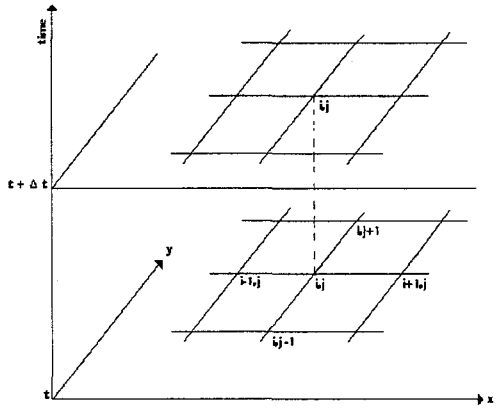

Figure 2. Grid for time-marching technique.

$\left(\partial U/\partial t\right)_{i,j}^{t}$ is calculated using forward spatial differences on the right side of the governing equations from the known flow field variables at time t, so

$$\left(\frac{\partial U}{\partial t}\right)_{i,j}^{t} = -\frac{E_{i+1,j}^{t} - E_{i,j}^{t}}{\Delta x} - \frac{F_{i,j+1}^{t} - F_{i,j}^{t}}{\Delta y} \tag{10}$$

The predicted values of the flow field variables can be obtained at time $t + \Delta t$ as follows

$$\overline{U}_{i,j}^{t+\Delta t} = U_{i,j}^{t} + \left(\frac{\partial U}{\partial t}\right)_{i,j}^{t} \Delta t \tag{11}$$

$\left(\partial \overline{U}/\partial t\right)_{i,j}^{t+\Delta t}$ is calculated using backward spatial differences on the right side of the governing equations from the known flow field variables at time $t + \Delta t$,

$$\left(\frac{\partial \overline{U}}{\partial t}\right)_{i,j}^{t+\Delta t} = -\frac{\overline{E}_{i,j}^{t+\Delta t} - \overline{E}_{i-1,j}^{t+\Delta t}}{\Delta x} - \frac{\overline{F}_{i,j}^{t+\Delta t} - \overline{F}_{i,j-1}^{t+\Delta t}}{\Delta y} \tag{12}$$

The average time U-derivative $\left(\partial\overline{U}/\partial t\right)_{av}$ now can be computed and the values of the flow field variables are obtained.

In order to keep a second-order-accuracy for MacCormack's technique, the forward and backward differences are used for all spatial derivatives in the predictor and corrector steps respectively.

In the predictor step the x-derivatives and y-derivatives appearing in the viscous terms (viscous shear forces and heat conduction) in E must use backward and central-differences, respectively. While the x-derivatives and y-derivatives appearing in the viscous terms in F must use central and backward-differences, respectively.

In the corrector step the x-derivatives and y-derivatives appearing in the viscous terms in E must use forward and central-differences, respectively. While the x-derivatives and y-derivatives appearing in the viscous terms in F must use central and forward-differences, respectively.

The predictor and corrector steps are repeated until the flow field variables approach a steady-state value. For this purpose the densities at each point between two consecutive steps are tested, and if the differences is less than a specific tolerance, a steady-state value is assumed.

For starting MacCormack's time marching technique, initial conditions are needed, and the free-stream values are placed for all variables. Also, the explicit MacCormack's technique requires a limitation on the time step to ensure numerical stability. MacCormack[21] suggests

$$\left(\Delta t_{CFL}\right)_{i,j} = \left[\frac{\left|u_{i,j}\right|}{\Delta x} + \frac{\left|v_{i,j}\right|}{\Delta y} + a_{i,j}\sqrt{\frac{1}{\Delta x^2} + \frac{1}{\Delta y^2}}\right]$$

$$+2\max\left[\frac{4\left(\gamma\mu_{i,j}/\mathrm{Pr}\right)}{3\rho_{i,j}}\right]\left(\frac{1}{\Delta x^2} + \frac{1}{\Delta y^2}\right)\Bigg]^{-1} \qquad (13)$$

where $\Delta t = \min\left[K\left(\Delta t_{CFL}\right)_{i,j}\right]$

for only internal grid points with $0.5 \le K \le 0.8$.

RESULTS

For this specific problem, air will be considered as a perfect gas with the following properties:

$\gamma = 1.4$, R= 287 kg/J K, Pr= 0.71.

For all time the boundary conditions of the problem are

$u(0,0,t) = 0$	stagnation point;
$u(x \neq 0,0,t) = 0$	no slip conditions;
$v(x,0,t) = 0$	non-porous wall;
$T(x \neq 0,0,t) = T_w$	constant wall temperature;
$u(x,\infty,t) = u_\infty$	free stream velocity;
$T(x,\infty,t) = T_\infty$	free stream temperature.

The computational code was first validated by comparing with Anderson's[11] results where free stream conditions for pressure and temperature at the leading edge were also assumed,

$p(0,0,t)=p_\infty$ $T(0,0,t)=T_\infty$.

Figures 3 and 4 describe the distribution of the normalized pressure along the plate at Mach number 4 for wall to free-stream temperature ratios 1 and 3, respectively. The transverse distribution of normalized pressure, temperature, density and the streamwise velocity at the cross section $x=10^{-5}$ (m) are presented in Figures 5 and 6, respectively. The nonlinear shock wave-boundary layer interaction is evident, resulting in complicated distributions of the pressure and temperature. Results presented in the Figures 3 and 5 nicely agree with Anderson's results.[11]

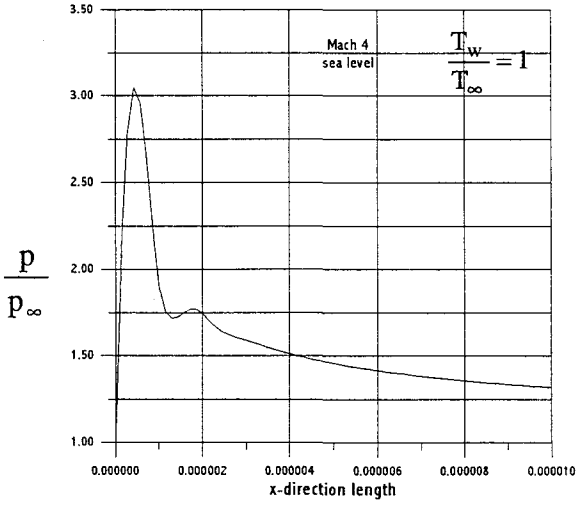

Figure 3. Pressure distribution in x-direction.

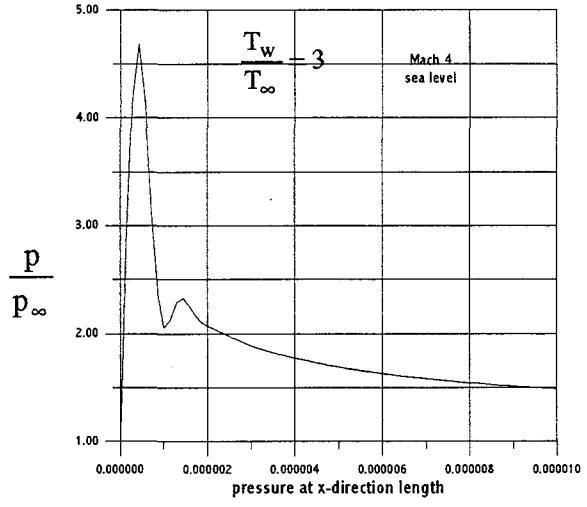

Figure 4. Pressure distribution in x-direction.

It can be seen that for both flow cases with Mach number 4 ($\frac{T_w}{T_\infty} = 1$ and $\frac{T_w}{T_\infty} = 3$), the shock wave and boundary layer do not merge. Also, at the trailing edge of the plate, the pressures in both the x-direction (Figures 3 and 4) and the y-direction (Figures 5 and 6) are nearly constant inside the boundary layer and both pressure gradients may be neglected, $\frac{\partial p}{\partial x} = \frac{\partial p}{\partial y} = 0$.

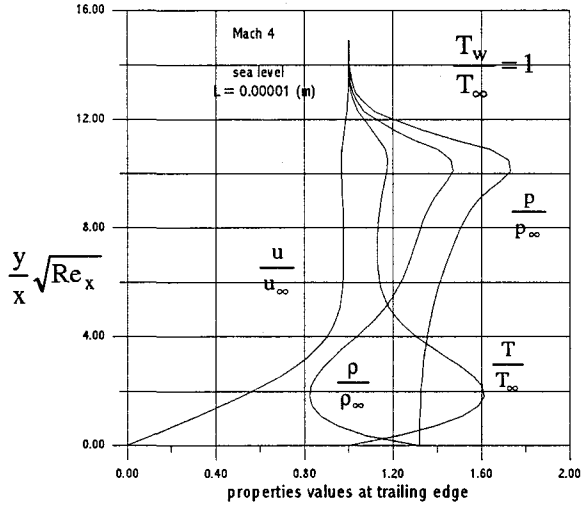

Figure 5. Streamwise velocity, pressure, temperature and density.

However, outside the boundary layer in the region between the boundary layer and the shock wave, the pressure distribution in the y-direction is not constant and there $\frac{\partial p}{\partial y} \neq 0$ but $\frac{\partial p}{\partial x} = 0$. Therefore, we conclude that in the cases studied above the classical self-similar boundary layer equations may be used near the trailing edge of the plate.

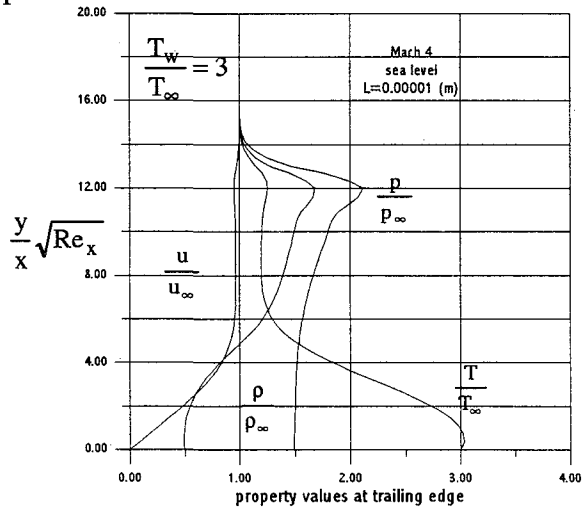

Figure 6. Streamwise velocity, pressure, temperature and density.

We used the approach of Toro et al.[18] to compute the self-similar boundary layer structure for the case $M_\infty = 4$ and $\theta_w = \frac{T_w}{T_\infty} = 3.0$. Figure 7 presents the results for the streamwise velocity and temperature profiles at Mach number 4. Here we used the power $\alpha = 0.63$ as the power in the viscosity-temperature relation which best matches Sutherland's law.

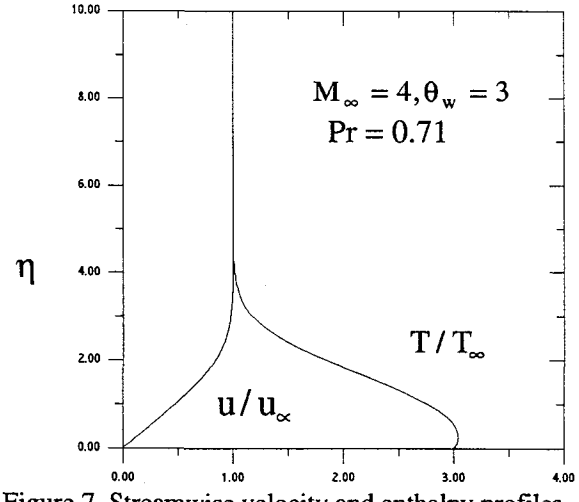

Figure 7. Streamwise velocity and enthalpy profiles.

In Figure 8 we compare the temperature profiles computed at the plate trailing edge, as given in Figure 6, with two possible similarity solutions. One, where the temperature T at the boundary layer edge equals T_∞, and the other, where it is 1.2 T_∞. It can be seen that both similarity solutions nicely predict the boundary layer thickness and the temperature increase inside the boundary layer as computed by the complete viscous solution.

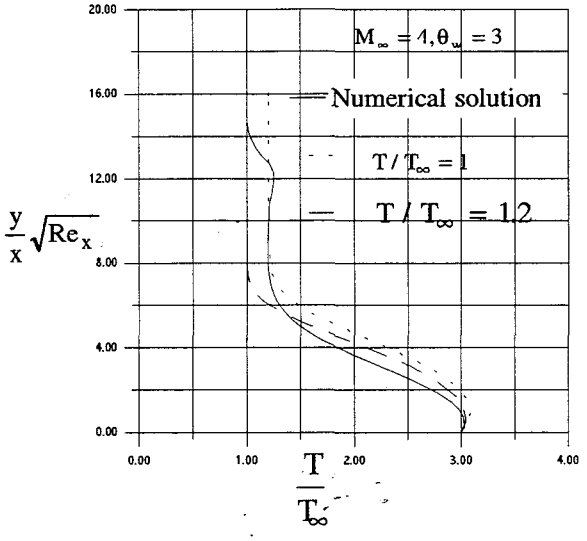

Figure 8. Streamwise velocity and enthalpy profiles.

Figures 9 to 11 show the results when the free stream Mach number is 15 using the finite difference and MacCormack's technique. The pressure distribution along the plate is given in Figure 9. At the trailing edge both $\frac{\partial p}{\partial y}$ and $\frac{\partial p}{\partial x}$ are not negligible, see Figures 9 and 10. Also, in this case both the shock wave and the boundary layer are merged all over the plate, as Nagamatsu et al.[5, 6, 9, 12] showed in their previous experimental and numerical results.

The streamwise velocity and temperature profiles using the self-similar solutions[18] at Mach number 15 are presented in Figure 11.

The increase in the temperature inside the boundary layer calculated by the similar solution, agrees nicely with the numerical results. In both cases, $\frac{T_{max}}{T_\infty} \approx 11$ (see Figures 10 and 11). However, the boundary layer thickness according to the self-similar solution is over predicted (see Figure 12), since in the numerical solutions presented the boundary layers are still within the strong interaction region and does not establish yet a self-similar structure.

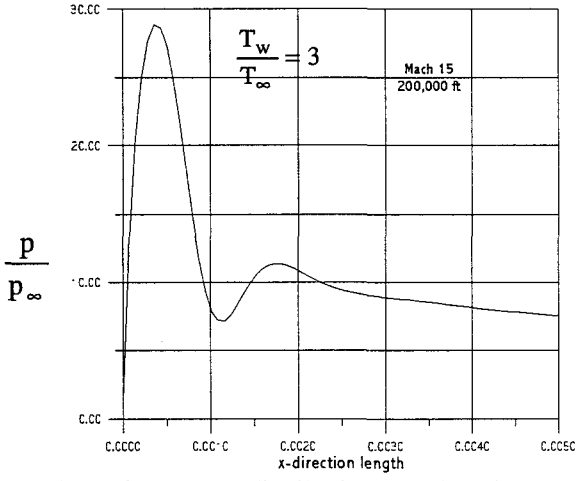

Figure 9. Pressure distribution in x-direction.

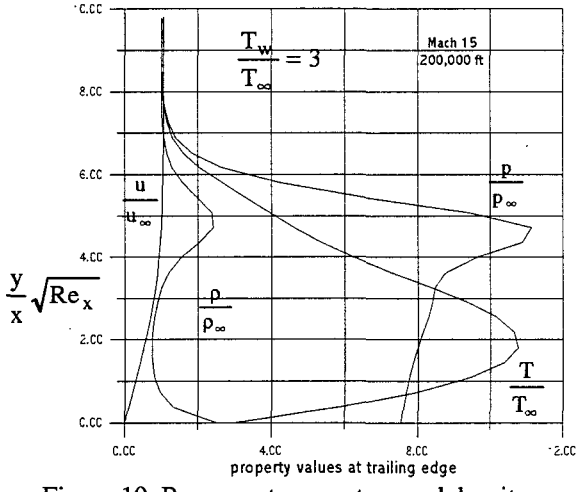

Figure 10. Pressure, temperature and density.

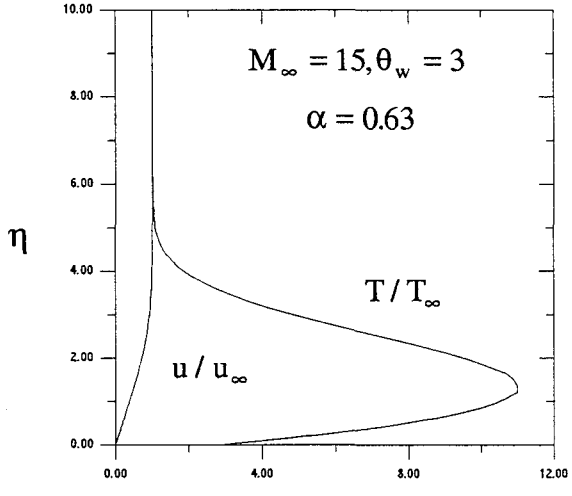

Figure 12. Streamwise velocity and enthalpy profiles.

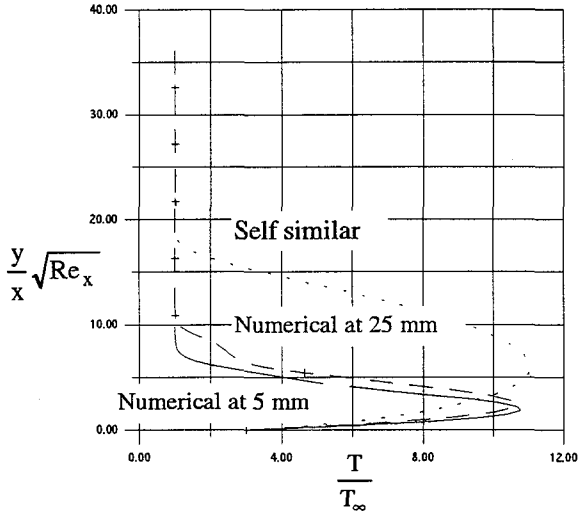

Figure 12. Temperature profiles.

Figure 13 presents the distribution of the computed induced normalized pressure along the flat plate at M_∞ =15.2 and T_0 = 1300 K for three different meshes. Figure 14 describes the transverse distribution of the normalized density ratio at the trailing edge of the plate for a various meshes. It can be seen that the grid refinement results in numerical solutions that tend to converge. The strong nonlinear interaction between the shock wave and the boundary layer is evident from these figures and results in very high pressure close to the leading edge of the plate.

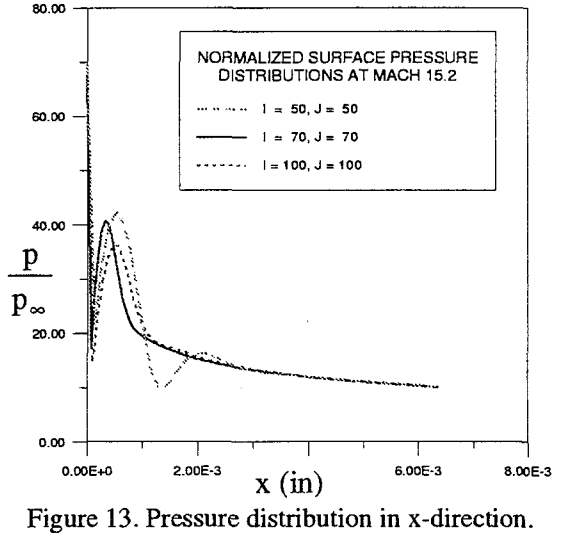

Figure 13. Pressure distribution in x-direction.

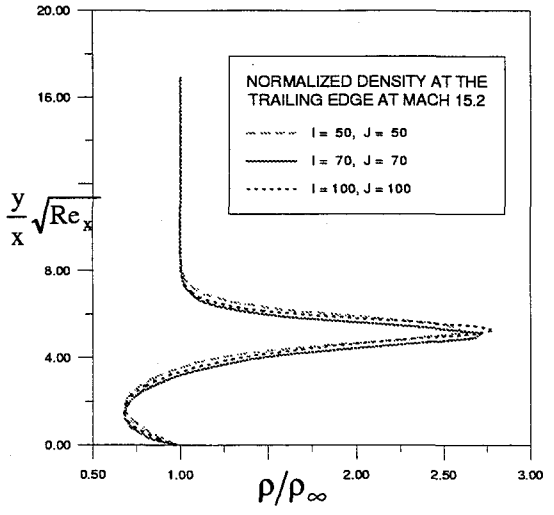

Figure 14. Density distribution in y-direction.

CONCLUSIONS

The interactions between a shock wave and a boundary layer, near the leading edge of a flat plate, in supersonic and hypersonic viscous flow are numerically investigated. The full two-dimensional Navier-Stokes equations are solved by the explicit finite-difference MacCormack's time marching technique.

Solutions for the flow parameters such as the boundary layer thickness, the pressure profile in both directions (x and y directions), the streamwise velocity profile and the temperature and density distributions over a flat plate with constant surface temperature are presented.

The numerical results are compared with recent similarity solutions for supersonic laminar boundary layers that use a general power law for the viscosity-temperature relation. Nice agreement between solutions is found at the trailing edge of the plate. It seems, however, that a longer plate is needed for the flow to establish a self-similar structure as Mach number is increased.

ACKNOWLEDGMENTS

This report was prepared under contract No. NCC8-112 for NASA Marshall Space Flight Center. The first author wishes to thank the Brazilian Foundation (FAPESP) for supporting his graduate studies, and the Aeronautic and Space Institute (IAE) which allowed him to pursue graduate studies at Rensselaer Polytechnic Institute (RPI) Also he would like to thank Manoel E. M. de Carvalho for

helping him in several occasions through invaluable discussions on aspects related to this paper.

REFERENCES

1. Sternberg, J. "A Free-Flight Investigation of the Possibility of High Reynolds Number Supersonic Laminar Boundary Layers," J. Aero. Sci., vol. 19, n. 11, pp. 721-733, Nov. 1952.
2. Van Driest, E.R., "Calculation of the Stability of the Laminar Boundary Layer in a Compressible Fluid on a Flat Plate with Heat Transfer," ," J. Aero. Sci., vol. 19, n. 12, pp. 801-812, Dec. 1952.
3. Schaaf, S.A.; Hurlbut, F.C.; Talbot, L.; Aroesty, J. Viscous interaction experiments at low Reynolds number. ARS J., vol. 29, no. 7, pp. 527-528, 1959.
4. Laurmann, J. A. The effect of slip on induced pressures. J. Aero/Space Sci., vol. 26, no. 1, pp. 53-54, 1959.
5. Nagamatsu, H. T.; Sheer, R.E., Jr. Hypersonic shock wave-boundary layer interaction and leading edge slip. ARS J., vol. 30, no. 5, pp. 454-462, 1960.
6. Nagamatsu, H.T. and Li, T.Y. Hypersonic Flow near the Leading Edge of a Flat Plate. The Physics of Fluids 3, no. 1, pp. 140-141, 1960.
7. Hammitt, A.G.The hypersonic viscous effects on a flat plate with finite leading edge. J. Fluid Mech., vol. 5, no. 2, pp. 242-256, 1959.
8. Cheng, H.K.; Hall, J.G.; Golian, T.C.; Hertzberg, A. Boundary layer displacement and leading edge bluntness effects in high temperature hypersonic flow. J. Aero/Space Sci., vol. 28, no. 5, pp. 353-381, 1961.
9. Li, T.Y.; Nagamatsu, H.T. Shock wave effects on the laminar skin friction of and insulated flat plate at hypersonic speeds. J. Aeronautical Sci., vol. 20, no. 5, p. 345-355, 1953.
10. Kuerti, G., "The laminar boundary layer in compressible flow," Advances in Applied Mechanics II, Academic Press Inc., 1951.
11. Anderson, J.D.; Jr. Modern compressible flow, with historical perspective. MacGraw-Hill Book Co., 1990.
12. Li, T.Y.; Nagamatsu, H.T. Similar solutions of compressible boundary-layer equations. J. of Aeronautical Sciences, vol. 22, no. 9, pp. 607-616, 1955.
13. Li, T.Y.; Nagamatsu, H.T.Hypersonic viscous flow on noninsulated flat plate. Heat Transfer and Fluid Mechanics Institute, University of California, Los Angeles, June 1955.
14. Nagamatsu, H.T.; Messit, D.G.; Myrabo, L.N.; Sheer, R.E., Jr.Computational, theoretical and experimental investigation of flow over a sharp flat plate M_1 10 - 25. AIAA 94-2350, 25th AIAA Fluid Dynamics Conference, 1994.
15. Cooper, G.K. The PARC code: theory and usage. AEDC-TR-87-24, Arnold Engineering Development Center, 1987.
16. Moraes, A.C.M.; Flaherty, J.E.; Nagamatsu, H.T. A study of compressible laminar boundary layers at Mach numbers 4 to 30. AIAA 91-0323, 29th Aerospace Sciences Meeting, 1991.
17. Van Driest, E.R. "Investigations of Laminar Boundary Layer in Compressible Fluids using the Crocco Method," NACA TN 2597, 1952.
18. Toro, P.G.P; Rusak, Z; Nagamatsu, H.T; and Myrabo, L.N., "Self-Similar Compressible laminar Boundary Layers," AIAA 97-0767, 35th Aerospace Sciences Meeting and Exhibit, Reno, NV, 1997.
19. Toro, P.G.P; Rusak, Z; Nagamatsu, H.T; and Myrabo, L.N., "Self-Similar Compressible Laminar Boundary Layers Applied To A Shock Wave Advancing Into A Stationary Fluid," A, to be presented.
20. Anderson, D. A.; Tannehill, J. C. and Pletcher, R. H. Computational Fluid Mechanics and Heat Transfer. MacGrawhill 1984.
21. MacCormack, R.W. Current Status of Numerical Solutions of the Navier-Stokes Equations. AIAA paper 88-0513, 1988.